Electronic Supplementary Information (ESI)

Application of an inorganic sulfur-modified expanded graphite for sodium storage at low temperature

Li-Feng Zhou, [a] Yi-Jing Gao, [b] He Gong, [a] Li-Ying Liu [a] and Tao Du *[a]

Experimental

Synthesis of S-EG

All chemicals utilized in this work were purchased from Aldrich and were of analytical grade without further purification. Initially, graphene oxide was prepared by the improved Hummers method.[1] Then the black powder was heated highly to 850℃ at a heating-rate of 10 ℃ min^{-1} and kept for 30 min in the atmosphere of Ar, followed by a careful collection of expanded graphite (EG). EG and commercial sublimed sulfur with a mass ratio of 1:1 were fully mixed by ball-milling in Ar and then were placed a vacuum tube furnace in Ar. The heating process was divided into three parts, including 155 ℃ for 1h, 300℃ for 1h and 600 ℃ for 3h, respectively. Finally, expanded graphite expanded by few sulfur (S-EG) was carefully collected as a final sample.

Characterization

The phase analysis of the as-obtained products was characterized by a powder X-ray diffraction (XRD, Bruker D8 ADVANCE, Cu Kα radiation, λ= 0.154 nm) at 40 kV, collected in the 2θ range of 20~60° at a scanning speed of 5° min^{-1}. The morphologies and corresponding elemental mapping images were analyzed by scanning electron microscopy (SEM, Zeiss Ultra Plus, accelerating voltage: 15kV) and transmission electron microscopy (TEM, FEI Tecnai G2 F20, Accelerating voltage: 200kV). The element distribution was evaluated by X-ray photoelectron spectroscopy (XPS, Escalab 250 Xi) spectrum, using C 1s (Binding Energy: 284.6 eV) as a reference. N_2 adsorption/desorption isotherms were measured at liquid nitrogen temperature using ASAP 2460. Raman spectra were recorded on a Raman microprobe (HR800, HORIBA JY) with 632.8 nm laser excitation. Fourier transform infrared spectroscopy (FTIR) spectra were collected from a Cary 660 FTIR spectrometer (Agilent Technologies) with 32 scans at a resolution of 4 cm^{-1}. Thermogravimetric analysis (TGA) was performed under the Ar atmosphere with the heating rate of 5℃ min^{-1}.

Electrochemical measurements

Galvanostatic charge/discharge performance were tested by CR2032-type cells assembled in a glove box under the Ar atmosphere with the vapor and the oxygen content strictly below 0.1ppm. The working electrodes were prepared by mixing the as-prepared anodes with super P and polyvinylidene fluoride (PVDF) at a respective weight ratio of 7:2:1 in N-methyl pyrrolidone (NMP) solvent. The coin cells were assembled with 1 M sodium perchlorate ($NaClO_4$) in a mixture of ethylene carbonate/dimethyl carbonate (EC/DMC) solution (1:1 in volume ratio) with 5wt% fluoroethylene carbonate (FEC) as the electrolyte, and the glass fiber membrane was the separator. Cyclic voltammetry (CV) and electrochemical impedance spectroscopy (EIS) measurements were performed on a CHI660E electrochemical station and a PARSTAT 2273 . electrochemical station, respectively. CV was collected at the different scan rates (0.1-2.0 mV s^{-1}) from 0 to 2.5 V and the testing range of EIS was a perturbation voltage of 5 mV in the frequency range between 100 kHz and 0.01 Hz at room temperatures. Galvanostatic The cyclic and rate performances were tested in the voltage range of 0-2.5 V on Land CT2001A battery test system.

Computational details

Galvanostatic intermittence titration technique (GITT) technique was also tested by the LAND system. Before the test, the batteries were charged/discharged at 0.2C for ten cycles to age the batteries. The batteries were performed for 20

min interlarding with a 60 min relaxing time at 0.2C, which was used to calculate the Na^+ diffusion coefficient reflecting the kinetic behaviors of S-EG was calculated with the equation:

$$D_{GITT}=\frac{4}{\pi t}\left(\frac{m_B V_m}{M_B S}\right)^2\left(\frac{\triangle E_S}{\triangle E_t}\right)^2 \quad (3)$$

where D_{GITT} is the ion diffusion coefficient, t is the relaxing time of the current pulse, m_B is the mass of active materials, V_m is its molar volume ($cm^3\ mol^{-1}$), M_B is the molar mass ($g\ mol^{-1}$), S is the total contacting area of electrode with electrolyte, $\triangle E_s$ and $\triangle E_t$ signify the steady-state potential change by the current pulse and potential change during the constant current (V), which are eliminated with the iR drop.

The D_{Na^+} value can be determined according to the following Equation:

$$D_{Na^+}=\frac{R^2\times T^2}{2A^2\times n^4\times F^4\times C_{Na^+}^{\ 2}\times \sigma^2}$$

where R is the gas constant, T is the absolute temperature, A is the electrode area, n is the number of transferred electrons, F is the Faraday constant, C_{Na^+} is the Na^+ concentration, and σ is the coefficient of Warburg impedance which is the slope of Z_{re} *vs*. $\omega^{1/2}$ plots.

Table S1 Comparison of low temperature properties of common carbon materials

Materials	Temperature (℃)	Current density (mA g^{-1})	Specific capacity (mAh g^{-1})	Ref.
Se/graphene	-5	243	346	[5]
Hard carbon	0	50	167	
Carbon nanosheets derived from corncob	0	50	132	
Carbon nanosphere derived from glucose	0	50	17	

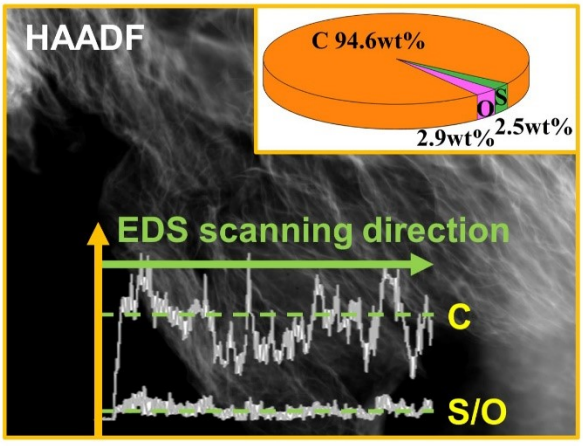

Figure S1 EDS line-scanning result based on a TEM-HAADF and element distribution ratio.

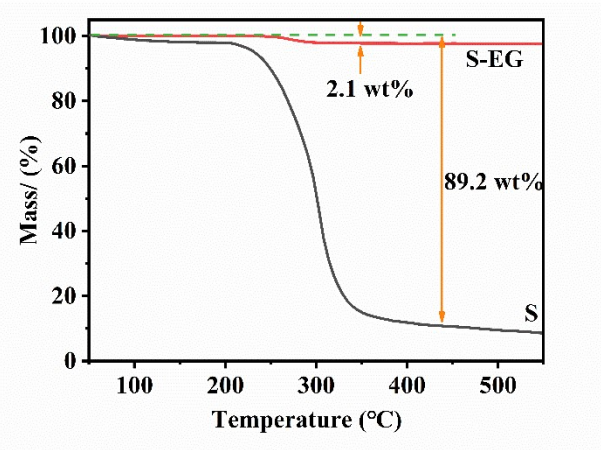

Figure S2 The mass loss of S-EG and S based on thermogravimetric analysis (TGA) under Ar atmosphere.

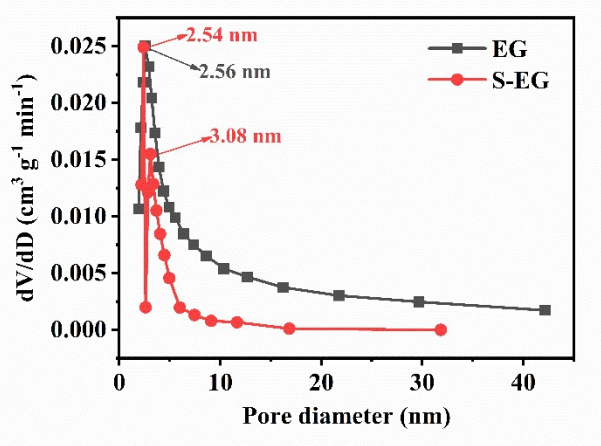

Figure S3 Pore distribution of EG and S-EG.

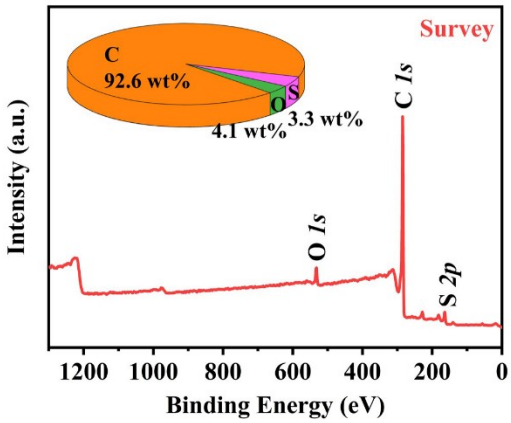

Figure S4 Survey scan spectrum contained the peaks of carbon, sulfur and oxygen, the inset was the element ratio

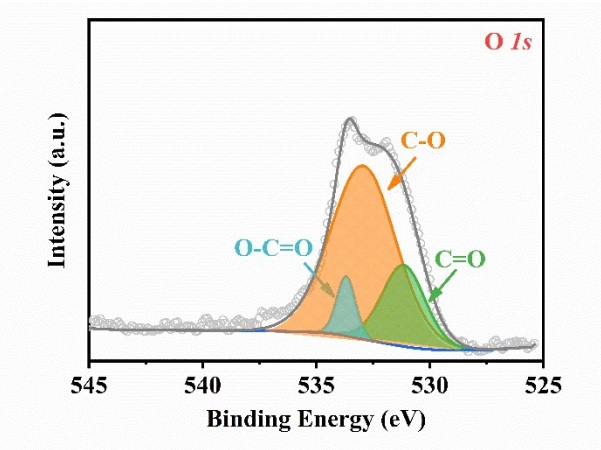

Figure S5 XPS high-resolution spectra of O *1s* for S-EG.

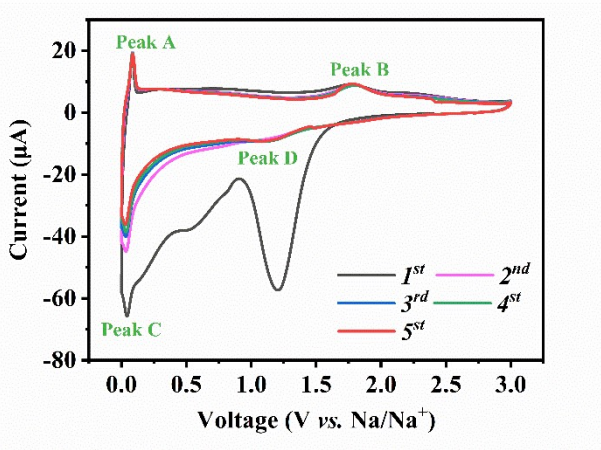

Figure S6 CV curves of the initial five cycles at 0.1 mV s^{-1} at LT..

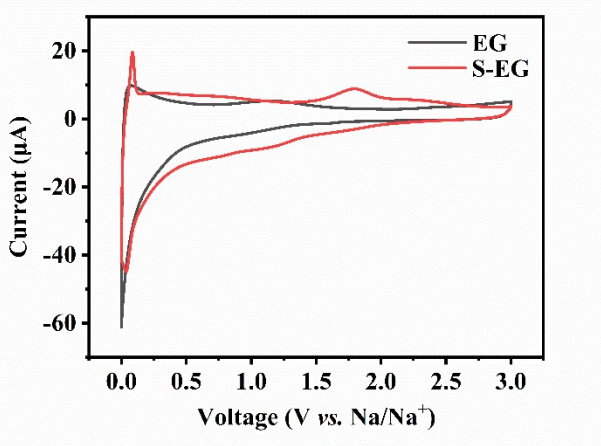

Figure S7 CV curves of EG and S-EG, respectively.

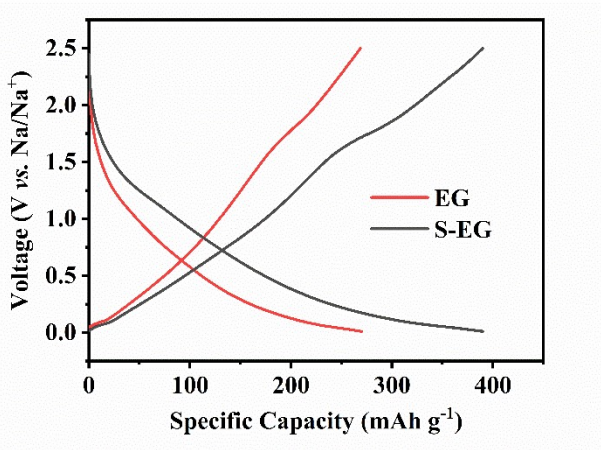

Figure S8 The 3rd charge and discharge profiles of EG and S-EG at 1.0C, respectively.

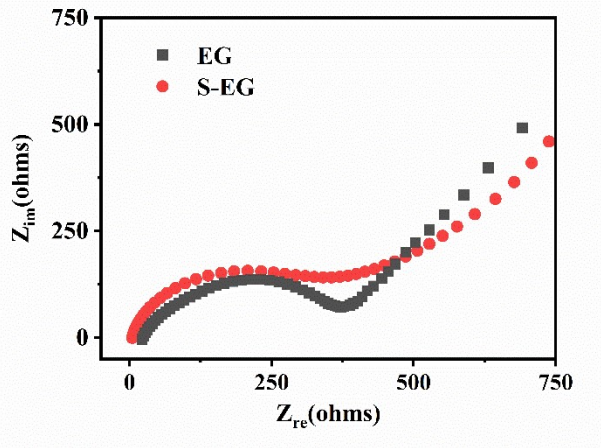

Figure S9 Nyquist plots of fresh cells employed EG and S-EG as anodes, respectively.

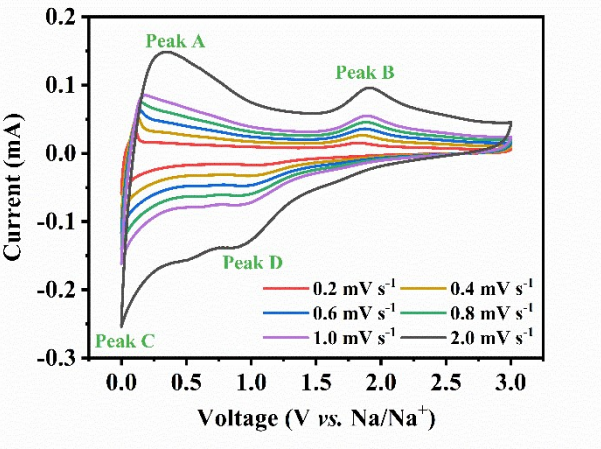

Figure S10 CV curves in the scan rate scope of 0.2 mV s^{-1} and 2.0 mV s^{-1}.

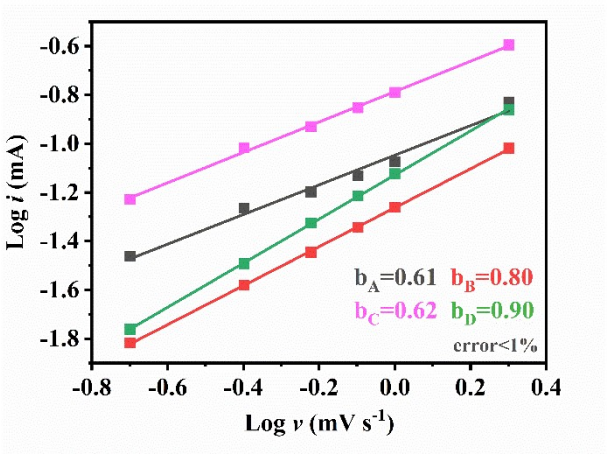

Figure S11 Plots of Log *i vs.* Log *v* calculated from CV curves and their fitting lines.

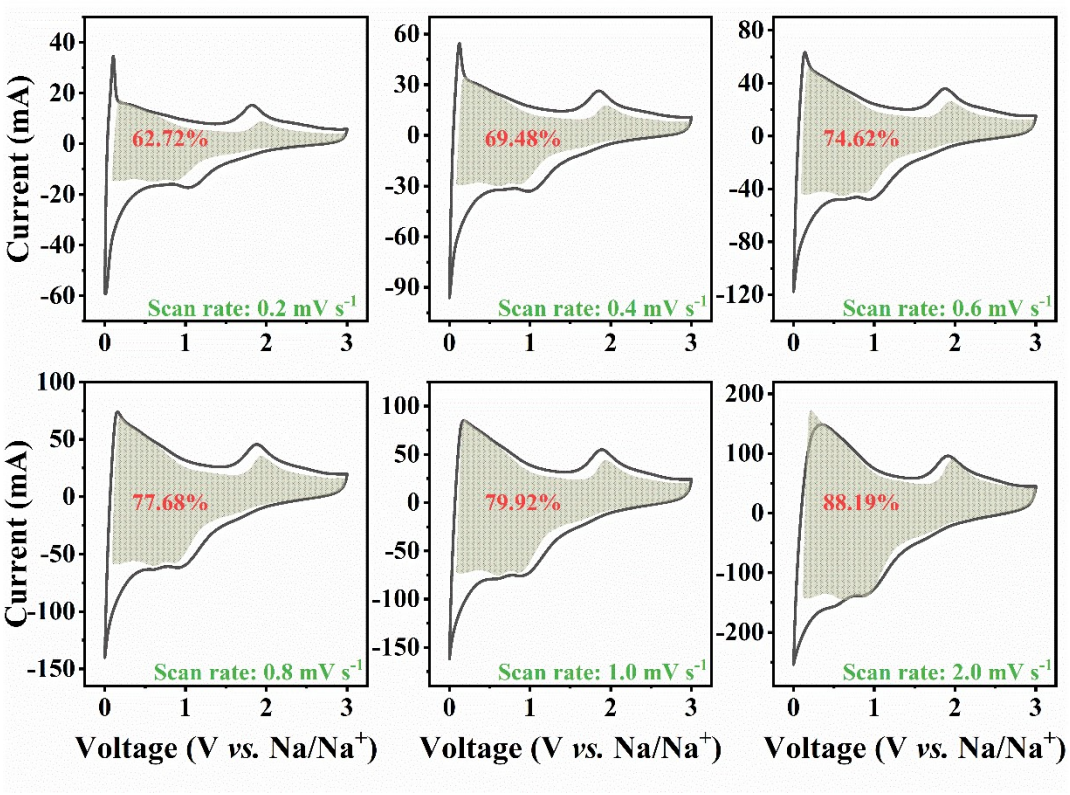

Figure S12 Calculated data of the capacitive control under various scan rates.

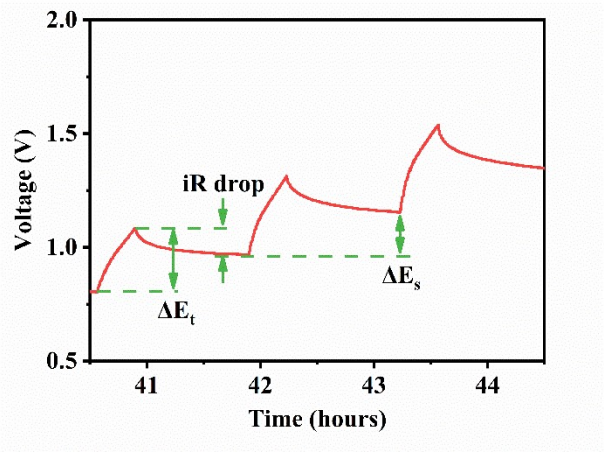

Figure S13 A voltage-time profile during a GITT measurement at 0.2C

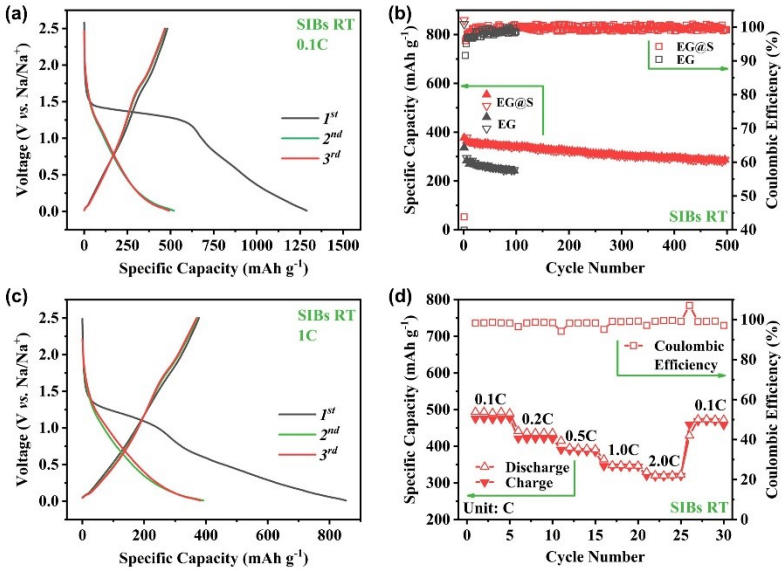

Figure S14 (a)Charge/discharge profiles of the initial three cycles at 0.1 C. (b) Cycle performance of S-EG and EG at 1C. (c) Charge/discharge profiles of the initial three cycles at 1 C (d) Rate performance of S-EG in the rate scope of 0.1 C and 2.0 C.

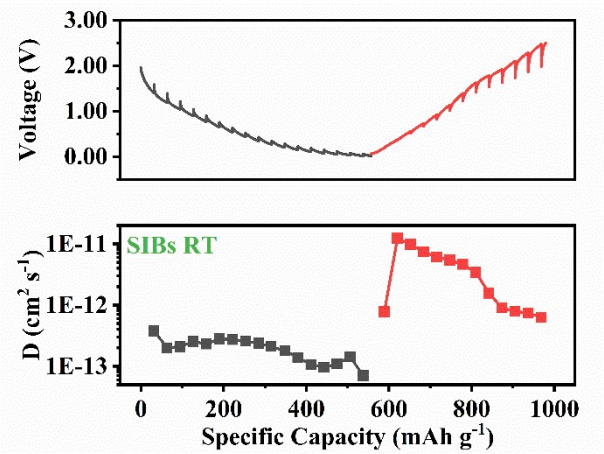

Figure S15 GITT curves and the calculate Na^+ diffusion coefficients

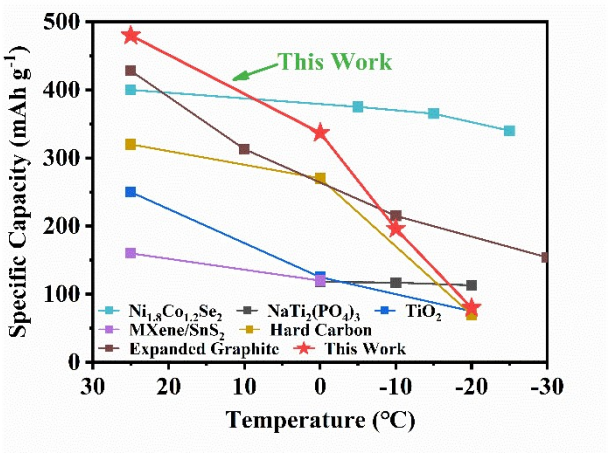

Figure S16 A comparison of the properties of this work with previously reported anode materials for SIBs at RT/LT.[2-7]

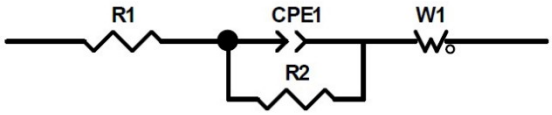

Figure S17 The fitting equivalent circuit.

Refence

[1] J. Chen, B. Yao, C. Li, G. Shi, Carbon 2013, 64, 225.

[2] B.-H. Hou, Y.-Y. Wang, D.-S. Liu, Z.-Y. Gu, X. Feng, H. Fan, T. Zhang, C. Lu, X.-L. Wu, Advanced Functional Materials 2018, 28.

[3] M. Kang, Y. Wu, X. Huang, K. Zhou, Z. Huang, Z. Hong, Journal of Materials Chemistry A 2018, 6, 22840.

[4] L. Wang, B. Wang, G. Liu, T. Liu, T. Gao, D. Wang, Rsc Advances 2016, 6, 70277.

[5] Y. Wu, P. Nie, L. Wu, H. Dou, X. Zhang, Chemical Engineering Journal 2018, 334, 932.

[6] X. Lin, X. Du, P. S. Tsui, J.-Q. Huang, H. Tan, B. Zhang, Electrochimica Acta 2019, 316, 60.

[7] L.-F. Zhou, H. Gong, L.-Y. Liu, Y.-S. Wang, T. Du, ChemNanoMat 2021.